grading the cognitive state of patients for the clinician. *J Psychiatr Res* 1975;12:189–198.
28. Mattis S. Mental status examination for organic mental syndrome in the elderly patient. In: Bellack L, Karasu TB, eds. *Geriatric psychiatry.* New York: Grune & Stratton; 1976:77–121.
29. Rosen WG, Mohs RC, Davis KL. A new rating scale for Alzheimer's disease. *Am J Psychiatry* 1984;141:1356–1364.
30. Wechsler D. *Wechsler adult intelligence scale—revised.* New York: Psychological Corporation; 1981.
31. Lassen NA, Sperling B. Technetium-99m-bicisate reliably images CBF in chronic brain diseases but fails to show reflow hyperemia in subacute stroke: report of a multicenter trial of 105 cases comparing $^{133}$Xe and $^{99m}$Tc-biscisate (ECD, Neurolite) measured by SPECT on same day. *J Cereb Blood Flow Metab* 1994;14:S44–S48.
32. Yonekura Y, Tsuchida T, Sadato N, et al. Brain perfusion SPECT with $^{99m}$Tc-biscisate: comparison with PET measurement and linearization based on permeablility-surface area product model. *J Cereb Blood Flow Metab* 1994;14:S58–S65.
33. Holm S, Madsen PL, Sperling B, Lassen NA. Use of $^{99m}$Tc-bicisate in activation studies by split-dose technique. *J Cereb Blood Flow Metab* 1994;14:S115–S120.
34. Genna S, Smith AP. The development of ASPECT, an annular single crystal brain camera for high efficiency SPECT. *IEEE Trans Nucl Sci* 1988;NS-35:654–658.
35. Holman BL, Carvalho PA, Zimmerman RE, et al. Brain perfusion SPECT using an annular single crystal camera: initial clinical experience. *J Nucl Med* 1990;31:1456–1461.
36. Kumar A, Schapiro MB, Grady C, et al. High-resolution PET studies in Alzheimer's disease. *Neuropsychopharmacology* 1991;4:35–46.
37. Matsui T, Hirano A. *An atlas of the human brain for computerized tomography.* Tokyo: Igaku-Shoin, Ltd; 1978.
38. Brun A, Englund E. Regional pattern of degeneration in Alzheimer's disease: neuronal loss and histopathological grading. *Histopathology* 1981;5:549–564.
39. Pearson RCA, Esiri MM, Hiorns RW, Wilcock GK, Powell TPS. Anatomical correlated of the distribution of the pathological changes in the neocortex in Alzheimer disease. *Proc Natl Acad Sci* 1985;82:4531–4534.
40. Rogers J, Morrison JH. Quantitataive morphology and regional and laminar distributions of senile plaques in Alzheimer's disease. *J Neurosci* 1985;5:2801–2808.
41. Fukuyama H, Ogawa M, Yamauchi H, et al. Altered cerebral energy metabolism in Alzheimer's disease: a PET study. *J Nucl Med* 1994;35:1–6.
42. Kushner M, Tobin M, AlaviA, et al. Cerebellar glucose consumption in normal and pathologic states using fluorine-18-FDG and PET. *J Nucl Med* 1987;28:1667–1670.
43. Herholz K, Perani D, Salmon E, et al. Comparability of FDG-PET studies in probable Alzheimer's disease. *J Nucl Med* 1993;34:1460–1466.
44. Herholz K, Adams R, Szelies B, Grond M, Heiss W-D. Criteria for the diagnosis of Alzheimer's disease with positron emission tomography. *Dementia* 1990;1:156–164.
45. Hanley JA, McNeil BJ. A method of comparing the areas under receiver operating characteristic curves derived from the same cases. *Radiology* 1983;148:839–843.
46. Morris J, McKeel D, Fulling K, Torack R, Berg L. Validation of clinical diagnostic criteria for Alzheimer's disease. *Ann Neurol* 1988;24:17–22.
47. Budinger TF, Derenzo SE, Greenberg WL, Guilberg GT. Quantitative potentials of dynamic emission computed tomography. *J Nucl Med* 1978;19:309–315.
48. Di Rocco RJ, Silva DA, Kuczynski BL, et al. The single-pass cerebral extraction and capillary permeability-surface area product of several putative cerebral blood flow imaging agents. *J Nucl Med* 1993;34:641–648.
49. Murase K, Tanada S, Inoue T, et al. Kinetic behavior of $^{99m}$Tc-ECD in the human brain using compartment analysis and dynamic SPECT: comparison with $^{99m}$Tc-HMPAO [Abstract]. *J Nucl Med* 1992;33(suppl):909.
50. Murase K, Tanada S, Inoue T, et al. Measurement of the blood-brain permeability of $^{123}$I-IMP, $^{99m}$Tc-HMPAO and $^{99m}$Tc-ECD in the human brain using compartment model analysis and dynamic SPECT [Abstract]. *J Nucl Med* 1991;32(suppl):911.
51. Moretti JL, Defer G, Tamgac F, Weinmann P, Belin C, Cesaro P. Comparison of brain SPECT using $^{99m}$Tc-bicisate (L,L-ECD) and [$^{123}$I]IMP in cortical and subcortical strokes. *J Cereb Blood Flow Metab* 1994;14:S84–S90.

# Brain SPECT Evaluation of Patients with Pure Photosensitive Epilepsy

L. Özlem Kapucu, Kivilcim Gücüyener, Gülin Vural, Gülsen Köse, Ayse Bora Tokçaer, Bülent Turgut and Mustafa Ünlü
*Departments of Nuclear Medicine, Pediatric Neurology and Neurology, Gazi University; and Department of Pediatric Neurology, Social Security Hospital, Ankara, Turkey*

This study was performed to determine the utility of $^{99m}$Tc-HMPAO brain SPECT in evaluating patients with pure photosensitive epilepsy. **Methods:** Seven patients (2 boys, 5 girls), aged 8 to 15 yr (mean 11.1 ± 2.5 yr), were studied. All patients underwent a detailed neurologic examination, interictal and ictal EEGs, CT and/or MRI and SPECT imaging. The baseline SPECT study was performed during the interictal period and the activation study was performed while the patients were having seizures provoked by watching television. **Results:** The baseline SPECT study showed that six of seven patients had relatively hypoperfused regions in their frontal lobes that could involve the neighboring parietal and temporal regions. The activation study revealed that all seven patients had relative hyperperfusion in these brain regions that were relatively hypoperfused in the baseline study. The side-to-side asymmetry indexes for these visually-interpreted rCBF abnormalities ranged from 3% to 6%. **Conclusion:** The relatively consistent pattern of frontal rCBF alterations suggests that frontal lobe functions were implicated in the evolution of photosensitivity-related seizures in patients with pure photosensitive epilepsy.

**Key Words:** pure photosensitive epilepsy; technetium-99m-HMPAO; brain SPECT; photic activation

**J Nucl Med 1996; 37:1755–1759**

Photosensitivity is found in 5% of epileptic patients and is associated with idiopathic generalized epilepsy, in which the prevalance may be as high as 25% (*1*). Forty percent of patients with seizures and photosensitivity have pure photosensitive epilepsy, in that all their attacks are visually precipitated and spontaneous seizures apparently do not occur (*1*). Seizures are commonly tonic-clonic (84% of this group, absences occur in 6%, partial seizures in 2.5% and myoclonic seizures in 1.5%). Nearly half of patients have a normal basic EEG, with abnormal activity occurring only on intermittant photic stimulation (IPS) (*1*).

The most common precipitant of seizures is television viewing. A more recent stimulus is the computer screen, although seizures may be induced by other sources of flickering light.

SPECT and PET functional neuroimaging techniques are used increasingly to diagnose seizure disorders, offering an accuracy of focus localization of approximately 90% for ictal and postictal studies in adult patients with complex partial seizures of temporal lobe origin (*2,3*). It has been suggested that $^{99m}$Tc-hexamethylpropylene amine oxime (HMPAO) SPECT scanning may be useful in early diagnosis of partial status epilepticus, especially in cases where the initial EEG and clinical symptoms are difficult to interpret (*4*). However, little is known about abnormalities in cerebral perfusion or metabolism in generalized seizures and photosensitivity-induced seizure disorders have not been studied with functional neuroimaging. The aim of this study was to determine the utility of $^{99m}$Tc-HMPAO brain SPECT in evaluating patients with pure photosensitive epilepsy.

Received Feb. 26, 1996; revision accepted March 6, 1996.
For correspondence or reprints contact: L. Özlem Kapucu, Department of Nuclear Medicine, Gazi University, Hoşdere Caddesi 3/17, Yukar[undot]i Ayranc[undot]i, 06540, Ankara, Turkey.

**TABLE 1**
Patient Clinical Data

| Patient no. | Age (yr) | Sex | Clinical seizure type | EEG (baseline) | EEG (watching TV) | CT/ MRI |
|---|---|---|---|---|---|---|
| 1 | 9 | F | Absence, bilateral myoclonus limited to eyelids | 8–9 Hz background | Diffuse polyspike discharges | Normal |
| 2 | 8 | M | Absence, bilateral myoclonus limited to eyelids | 8–9 Hz background | Diffuse polyspike discharges | Normal |
| 3 | 15 | M | Absence, bilateral myoclonus extending from eyelids to face | 9–11 Hz background | Diffuse spikewave and polyspike discharges | Normal |
| 4 | 12 | F | Absence, bilateral myoclonus extending from eyelids to face | 8–9 Hz background | Bilateral paroxysmal sharpwave, spike wave multiple spike wave predominantly parieto-occipital region | Normal |
| 5 | 9 | F | Absence, myoclonus involving the entire body bilaterally | 9–10 Hz background | Slow wave, spike wave polyspike discharges, bilateral parieto-occipital secondary bilateral generalization | Normal |
| 6 | 13 | F | Absence, myoclonus involving the entire body bilaterally | 8–9 Hz background | Diffuse polyspike discharges, bilateral frontal predominance | Normal |
| 7 | 12 | F | Absence, bilateral myoclonus limited to eyelids | 8–9 Hz background | Diffuse spike wave, polyspike discharges | Normal |

## MATERIALS AND METHODS

### Patients

Seven patients, ranging in age from 8 to 15 yr (mean 11.1 ± 2.5 yr), with histories of having seizures while watching television, were included in this study. All patients had seizures that started within a few weeks before admittance and were free of antiepileptic medication at the time of the SPECT study. Informed consent was obtained from parents for this investigation. Clinical examination of the patients during the interictal period was normal. All patients underwent EEG and CT and/or MRI examination (Table 1). After clinical and laboratory evaluation, all patients were diagnosed to have pure photosensitive epilepsy (PPE) with absence of type of seizure and myoclonic components to varying degrees (Table 1).

### Electroencephalogram

EEGs were recorded with an 8-channel apparatus through scalp electrodes (10–20 system). Six montages were used: two were monopolar and the others were bipolar. Table 1 shows the results of the EEG patterns.

### SPECT

An unstabilized version of $^{99m}$Tc-HMPAO was used as the perfusion agent. Commercially available kits were labeled according to the manufacturer's instructions. The SPECT study consisted of two steps: a baseline and an activation matrix.

*Baseline SPECT.* The baseline SPECT study was performed during the interictal period. Patients were injected intravenously with 297–370 MBq $^{99m}$Tc-HMPAO in a quiet room. Images of the head were acquired over 60 angles through 360°, with each angle being collected for 30 sec (dual-headed rotating gamma camera equipped with high-resolution collimator). Assessments were done with the patient in a quiet and semidark room with eyes open. Total acquisition time was approximately 30 min. Data were stored on a computer in a 64 × 64 matrix.

*Activation SPECT.* The activation study was performed on a separate day while the patients were watching television from a short distance to provoke seizures. Their EEGs were monitored at the same time. HMPAO was reconstituted by an experienced radiopharmacist according to manufacturer's instructions at the bedside after the start of television watching. The patient was injected with 297–370 MBq $^{99m}$Tc-HMPAO, prepared in advance, at the onset of seizures through a previously inserted two-way intravenous catheter. A sample of the injected material was collected at the time of injection and quality was checked. All patients had seizures that started less than 10 min from the onset of watching television and quality control checks revealed a labeling yield of 85% to 90% at the time of injection. Seizures lasted 15–20 sec on average and the patients continued to watch television for 3–4 min after recovering from the initial seizure. Some patients had additional seizures during this period. Repositioning of patients for the activation study was done carefully according to their previously recorded position during the baseline study with the help of a projected light source and bedside measurements. The lateral views of the baseline SPECT image (90° angle) were used as references to compare the slope of the orbitomeatal line. The SPECT study was performed with the same acquisiton parameters used for the baseline study.

Following image backprojection, image reconstruction was performed using Butterworth and ramp filters with an attenuation coefficient of 0.12, cutoff frequency of 0.39 and power factor of 10. Transaxial slices were obtained parallel to the orbitomeatal line. Transaxial, coronal and sagittal slices were generated in 6-mm pixels. Slices were analyzed visually and quantitatively.

### Visual Evaluation

Interpretation of the SPECT scans was performed qualitatively, by reviewing the images on a computer screen as well as on the recorded hard copy films, and independently by two experienced physicians who were blind to the EEG and structural imaging data. Disagreements were resolved by consensus.

An area was interpreted to show increased perfusion if the degree of uptake appeared substantially greater than that of adjacent and contralateral areas of the brain. Conversely, a region showing less uptake compared to adjacent and contralateral areas was considered hypoperfused. This type of subjective evaluation has proven accurate, particularly in patients with epilepsy (*4–7*). Additionally, regions in the activation study were compared with their counterparts in the baseline study. An area was reported as abnormal if this abnormality persisted on at least two adjacent slices.

### Quantitative Evaluation

The mean counts per pixel were calculated for 11 regions of interest (ROIs) on three representative transaxial slices. The lower slice displayed gray matter and orbitofrontal and temporal lobes. The middle slice displayed the frontal, parietal and occipital cortices. The higher slice was above the corpus callosum and displayed the frontal and parietal lobes. The slices were separated by three 18-mm pixels.

The slices were displayed on 128 × 128 matrices to minimize drawing errors. Eleven independent rectangular ROIs measuring 5 × 6 pixels were positioned manually over each area in each plane by visual inspection and isocount pixels around the cortex. These

**TABLE 2**
Results of Visual and Quantitative Evaluation

| Patient no. | Baseline | | Activation | |
|---|---|---|---|---|
| | Visual evaluation (Hypoperfusion) | Quantification (% Asymmetry) | Visual evaluation (Hyperperfusion) | Quantification (% Asymmetry) |
| 1 | Right frontal | −3 | Left frontal | +3 |
| | Right prefrontal | −3 | Left prefrontal | +3 |
| 2 | Left prefrontal | −3 | Left prefrontal | +4 |
| | Left frontoparietal | −3 | Left frontoparietal | +4 |
| | Right frontoparietal | −2 | Right frontoparietal | +4 |
| | Left frontotemporal | −3 | Left frontotemporal | +4 |
| | | | Left and right temporal | +3 |
| 3 | Left frontal | −3 | Left frontal | +4 |
| | Left prefrontal | −3 | Left prefrontal | +4 |
| 4 | Left frontoparietal | −2 | Left frontoparietal | +3 |
| | Left parietal | −3 | Left parietal | +4 |
| | | | Left parietotemporal | +3 |
| 5 | Left frontal | −3 | Left frontal | +5 |
| | Left prefrontal | −3 | Left prefrontal | +5 |
| | Left frontoparietal | −4 | Left frontoparietal | +5 |
| | Left frontotemporal | −4 | Left frontotemporal | +5 |
| | | | Left parietotemporal | +5 |
| | | | Left temporal | +5 |
| 6 | Normal | 0 | Anterior frontal | +6 |
| | | | Left and right frontal | +6 |
| | | | Left and right prefrontal | +6 |
| | | | Left and right frontoparietal | +6 |
| 7 | Left prefrontal | −3 | Left prefrontal | +4 |

were rotated to best follow the cortical outline and then mirrored across the midline, with minor lateral adjustments if necessary, to obtain the count density in the corresponding regions of the contralateral hemisphere. The same baseline set of ROIs was used for the activation study.

Count density was calculated for each ROI and the asymmetry from their counterparts in the opposite hemisphere and from adjacent anotomical regions of the same hemisphere were expressed as follows:

$$\% \text{ asymmetry index} = 100 \times (\text{right} - \text{left})/(\text{right} + \text{left}) \times 0.5.$$

## RESULTS

Visual evaluation of the baseline study showed that six of the seven patients had a detectable abnormality in regional cerebral blood flow during the interictal period (Table 2, Fig. 1). These abnormalities consisted of relative hypoperfusion in bilateral frontal, prefrontal, frontoparietal and left frontotemporal and parietal regions.

Visual evaluation of the SPECT images taken during television watching showed that all patients had abnormalities detected as relatively hyperperfused brain regions, including the anterior frontal, bilateral frontal, prefrontal, frontoparietal, frontotemporal, parietal, temporal and left parietotemporal regions (Table 2, Fig. 1). These hyperperfused regions occupied larger areas than baseline hypoperfused regions (Fig. 2) and were at the same localization except in Patient 6, whose baseline was normal (Fig. 3), and in Patient 1, whose hypoperfused and hyperperfused prefrontal regions were at the opposite hemispheres.

Quantitative evaluation showed that side-to-side asymmetry indices ranged between 3%–6% (Table 2). EEG recordings taken during television watching and the ictal period had a relatively common pattern of multifocal paroxysmal nonlocalized abnormalities with myoclonic features (Table 1). In two patients, a generalized epileptic pattern was preceded by bilateral parieto-occipital discharges by 1–2 sec. However, these were not considered as a focus.

## DISCUSSION

There is lack of agreement over what may be considered abnormal in tracer uptake between symmetrical regions in opposite hemispheres. Stapleton et al. (*8*) assessed the level at which trained human observers deemed single-focal count asymmetries to be clinically significant. They found that a rather severe defect (5%–10%) was required for detection. If such severe deficits were required in clinical practice, the sensitivity of scanning in mild disease would be quite poor. Although count reductions in individual regions of the brain may differ only marginally from normal, recognition of a typical clinical pattern of deficits can result in a confident diagnosis (*9*). Therefore, we looked for an identifiable SPECT pattern in our patients with PPE, and certain findings suggested the presence of it.

In the baseline interictal study, six of seven patients showed hypoperfusion in at least one of the regions of the frontal lobe. The patient who had no abnormality in frontal lobe images had a normal brain scan. The neighboring regions of parietal and temporal lobes were also hypoperfused in three and two patients, respectively. The pattern of interictal images, therefore, was hypoperfusion in frontal regions either on one side or bilaterally, sometimes including the neighboring parietal or temporal regions.

In the activation ictal study, all seven patients showed hyperperfusion in at least one of the regions of the frontal lobe. Ictal hyperperfusion tended to occupy larger areas than interictal hypoperfusion and was more likely to involve neighboring parietal and temporal regions. Ictal hyperperfusion was on the same side of interictal hypoperfusion in five of seven patients.

In one patient, hypoperfusion was on the right side, hyperperfusion being on the opposite side. The remaining patient had a normal baseline interictal scan. As seen from these findings, ictal images were also suggestive of an identifiable pattern for

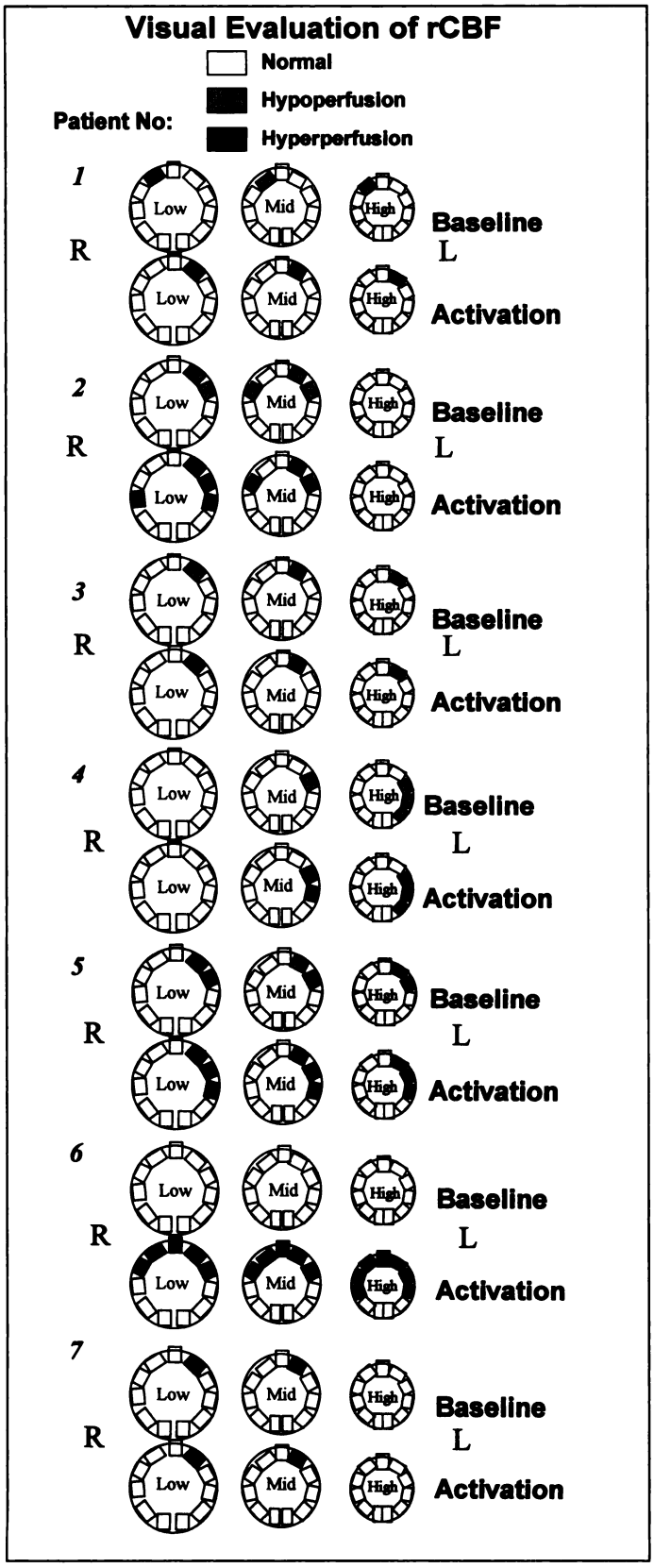


**FIGURE 1.** Visual evaluation of rCBF in patients with PPE. Schematic representation of the low, middle and high transaxial slices of baseline and activation SPECT images for individual patients.

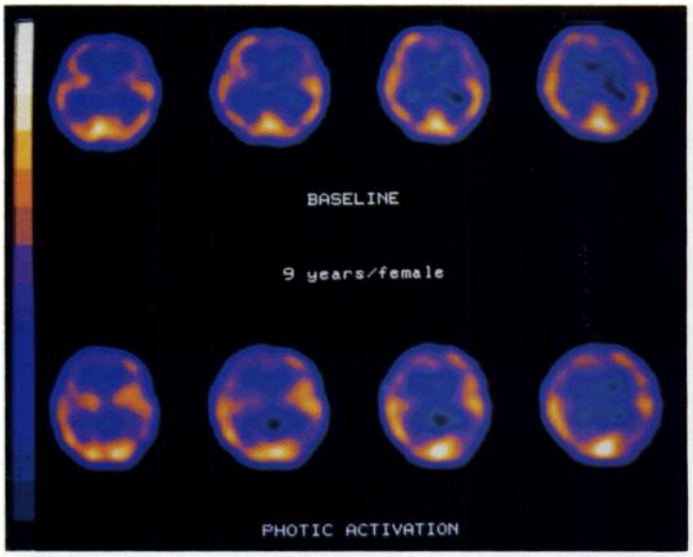


**FIGURE 2.** Sequential transaxial slices of Patient 5. Upper row: baseline study; relative hypoperfusion in left prefrontal, frontotemporal and frontoparietal regions. Lower row: activation study; relative hyperperfusion in left prefrontal, frontoparietal, frontotemporal, parietotemporal and temporal regions.

patients with PPE, its most prominent feature being hyperperfusion in the frontal regions.

Interictal EEG recordings of our patients were interpreted as normal, and ictal EEG findings did not indicate a focal frontal pathology. It was interesting to note that SPECT images revealed a pattern that was more like complex partial seizure disorders, although the EEG findings of our patients were typical of a generalized seizure disorder.

In their PET study of generalized seizure disorders, Theodore et al. (*10*) found that interictal glucose metabolism was normal in eight of nine patients. In their SPECT study, Devous et al. (*11*) found interictal hypoperfusion in only 3 of 15 patients, while Leroy et al. (*12*) found mild frontal rCBF abnormalities in 11 of 24 patients. In partial complex seizures of temporal and frontal lobe origin, the epileptic zone is hypoperfused during the interictal period (*13–16*) and hyperperfused during the ictal period (*13,16*). This sequence of events was observed in our patients with PPE.

Our limited understanding of the pathophysiology of photosensitive epilepsies has been increased by studies performed in the Papio papio baboon, which is the only natural experimental

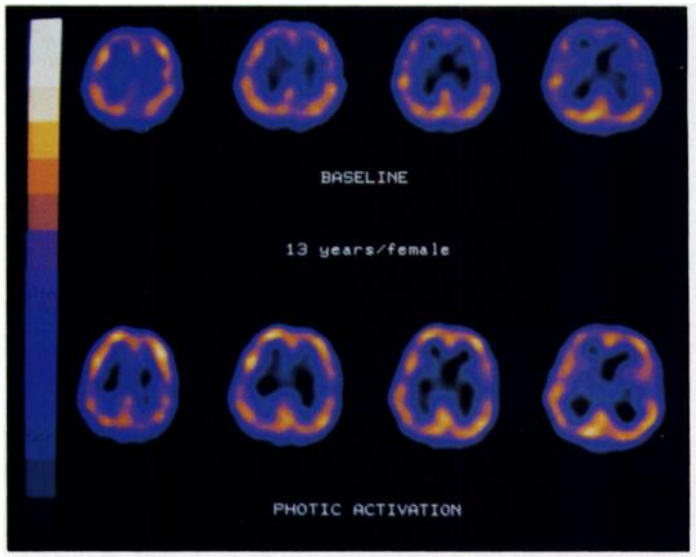


**FIGURE 3.** Upper row: baseline study; sequential transaxial slices of Patient 6 show normal perfusion. Lower row: activation study; sequential transaxial slices of the same patient show relative hyperperfusion in all frontal cortex regions.

model resembling human photosensitive epilepsy (*17–19*). It was demonstrated in photosensitive baboons, under IPS, that the frontal cortical neurons were progressively activated before paroxysmal discharges could be distinguished in the surface EEG recordings (*20*). As soon as the discharges were constituted, each burst became synchronous with a positive spike. The activation bursts of frontal neurons and the paroxysmal discharges were reversible and stopped when IPS ended.

In other cortical and subcortical structures, unitary and multiunitary recordings have shown a cellular activation only when frontal paroxysmal discharges have reached sufficent amplitude (*21*).

Silva-Barret et al. (*22*) demonstrated that generators of paroxysmal discharges were localized in the frontal cortex by performing a current-source density study in Areas 4 and 6 in photosensitive baboons submitted to IPS. A bilateral chronic infusion (7 days) of GABA into the motor cortex (Area 4) of photosensitive baboons completely blocked both the EEG and the clinical manifestations induced by IPS during the entire infusion period (*23*). A similar infusion performed in the occipital cortex was equally efficient, but infusions in Areas 6 and 8 had no effect. These results confirmed, first, that generators of epileptic manifestations in baboons were situated in the motor cortex and, second, that the visual afferents coming from the occipital cortex were necessary to trigger these generators (*24*).

In photosensitive patients, IPS was reported to induce spikes and waves that were localized occipitally in 59% of cases (*25*). Their existence indicated that changes in the excitability of the occipital cortex may be implicated in the mechanisms of photosensitive epilepsy. When paroxysmal discharges in photosensitive patients do not have an occipital origin, the characteristics of EEG and myoclonic discharges are very similar to those observed in baboons (*26*).

For primary generalized epilepsy in human patients, as with photosensitive epilepsy in baboons (*27*), no anatomical lesion has been observed in the frontal cortex that serves to explain its reactivity to IPS. Similarly, no anatomical lesion or functional anomaly of the visual system has been detected.

We did not observe any change in rCBF to occipital regions in any patient during interictal and ictal studies. This finding was in accordance with those obtained in electrophysiologic studies perfermed on baboons, which showed that the occipital cortex was not the primary area where the bulk of electrical activity occurs during IPS. This finding does not rule out a probable implication of the occipital cortex in the generation of photosensitive seizures, since a nerve impulse might be triggering the events but may be too small to cause metabolic changes that can be detected by neuroimaging methods. The rCBF alterations in the frontal regions of patients with PPE were probably reflections of the pathologic events taking place in these cortical areas during, or even before, the generation of seizures.

## CONCLUSION

The relatively consistent pattern of frontal rCBF alterations demonstrated in patients with PPE suggests that altered frontal lobe functions may be implicated in the evolution of photosensitivity-related seizures in humans.


## ACKNOWLEDGMENT

This paper was presented at 42nd Annual Meeting of the Society of Nuclear Medicine in Minneapolis, MN, June 1995.


## REFERENCES


1. Binnie CD, Jeavons PM. Photosensitive epilepsies In: Roger J, Bureau M, Dravet C, et al., eds. *Epileptic syndromes in infancy, childhood and adolescence*, 2nd ed. London: John Libbey and Co., Ltd.; 1992:299–305.
2. Shen W, Lee BI, Park HM, et al. HIPDM-SPECT brain imaging in the presurgical evaluation of patients with intractable seizures. *J Nucl Med* 1990;31:1280–1284.
3. Rowe CC, Berkovic SF, Sia STB, et al. Localization of epileptic foci with postictal SPECT. *Ann Neurol* 1989;26:660–668.
4. Tatum WO, Alavi A, Stecker MM. Technetium-99m-HMPAO SPECT in partial status epilepticus. *J Nucl Med* 1994;35:1087–1094.
5. Marks DA, Katz A, Hoffer P, Spencer SS. Localization of extratemporal epileptic foci during ictal SPECT. *Ann Neurol* 1992;31:250–255.
6. Rowe CC, Berkovic SF, Austin MC, et al. Patterns of postictal cerebral blood flow in temporal lobe epilepsy: qualitative and quantitative analysis. *Neurology* 1991;41: 1096–1103.
7. Lee BI, Markand ON, Wellman HN, et al. HIPDM SPECT brain imaging in partial-onset secondarily generalized tonic-clonic seizures. *Epilepsia* 1987;28:305–311.
8. Stapleton SJ, Caldwell CB, Leonardt CL, et al. Determination of thresholds for detection of cerebellar blood flow deficits in brain SPECT images. *J Nucl Med* 1994;35:1547–1555.
9. Juni JE. Taking brain SPECT seriously: reflections on recent clinical reports in the Journal of Nuclear Medicine. *J Nucl Med* 1994;35:1891–1895.
10. Theodere WH, Brooks R, Margolin R, et al. PET in generalized seizures. *Neurology* 1985;35:684–690.
11. Devous MD Sr, Stokely EM, Bonte FJ. Quantitative imaging of regional cerebral blood flow by dynamic single-photon tomography. In: Holman BL, ed. *Radionuclide imaging of the brain*. New York, NY: Churchill-Livingstone; 1985:135–161.
12. Leroy RF, Devous MD, Ajmani AK, et al. Regional cerebral blood flow determined by $^{133}$Xe inhalation and SPECT scan among epileptics with primary generalized seizures. *Neurology* 1987;37(suppl 1):102.
13. Duncan R, Patterson J, Roberts R, et al. Ictal/postictal SPECT in the pre-surgical localization of complex partial seizures. *J Neurol Neurosurg Psychiatry* 1993;56:141–148.
14. Andersen AR, a Rogvi-Hansen B, Dam M. Utility of interictal SPECT of rCBF for focal diagnosis of the epileptogenic zone(s). *Acta Neurol Scand* 1994;152(suppl):129–134.
15. Swartz BE, Theodore WH, Sanabria E, Fisher RS. Positron emission and single-photon emission computed tomographic studies in the frontal lobe with emphasis on the relationship to seizure foci. In: Chauvel P, Delgado-Escueta AV, et al., eds. *Advances in neurology*. New York, NY: Raven Press; 1992:487–497.
16. Grünwald F, Menzel C, Pavics L, et al. Ictal and interictal brain SPECT imaging in epilepsy using $^{99m}$Tc-ECD. *J Nucl Med* 1995;35:1896–1909.
17. Killam KF, Killam EK, Naquet R. Mise en évidence chez certains singes d'un snydrome myoclonique, C.R. *Acad Sci* (Paris) 1966;262:1010–1012.
18. Killam KF, Killam EK, Naquet R. Ėudes pharmacologiques réalisées chez des singes présentant une activité EEG paroxystique particulière à la stimulation lumineiuse intermittente. *J Physiol* (Paris) 1966;58:543–544.
19. Meldrum BS, Balzamo E, Gadea M, Naquet R. Photic and drug induced epilepsy in the baboon (Papio papio). The effect of isoniazid, thiosemicarbazide, pyridoxine and amino-oxyacetic acid. *Electroenceph Clin Neurophysiol* 1970;29:33–347.
20. Menini CH, Silva-Comte C, Stutzmann JM, Dimov S. Cortical unit discharges during photic intermittent stimulation in the Papio papio. Relationships with paroxysmal fronto-rolandic activity. *Electroenceph Clin Neurophysiol* 1981;52:42–49.
21. Silva-Barret C, Menini CH, Bryere P, Naquet R. Multiunitary analysis of cortical and subcortical stuctures in paroxysmal discharges and grand mal seizures in photosensitive baboons. *Electroenceph Clin Neurophysiol* 1986;64:455–468.
22. Silva-Barret C, Brailowsky S, Levesque G, Menini CH. Epileptic discharges induced by intermittent light stimulation in photosensitive baboons: a current source density study. *Epilepsy Res* 1988;2:1–8.
23. Menini C, Brailowsky S, Silva-Barrat C, et al. Cortical GABAergic control of epilepsy in photosensitive baboons. In: Chauvel P, Delgado-Escueta AV, et al., eds. *Advances in neurology*. New York, NY: Raven Press; 1992:571–578.
24. Silva-Barret C, Menini CH. The influence of light stimulation on potentials evoked by single flashes in photosensitive and nonphotosensitive Papio papio. *Electroenceph Clin Neurophysiol* 1984;57:448–461.
25. Takahashi T. Precipitation of photosensitive epileptic seizures. In: Akimoto H, Kasamatsuri M, Seino M, Ward AA, eds. *Advances in epileptology: the XIIIth Epilepsy International Symposium*. New York, NY: Raven Press; 1982: 255–259.
26. Menini CH, Naquet R. Les myoclonies. Des myoclonies du Papio papio à certaines myoclonies humaines. *Rev Neurol* (Paris) 1986;142:3–28.
27. Riche D, Gambarelli-Dubois DM, Naquet R. Repeated seizures and cerebral lesions in photosensitive baboons (Papio papio). A preliminary report. In: Brierley JB, Meldrum BS, eds. *Brain hypoxia*. London, England: Spactics Intern; 1971:297–301.